

# RSC Advances



This is an *Accepted Manuscript*, which has been through the Royal Society of Chemistry peer review process and has been accepted for publication.

*Accepted Manuscripts* are published online shortly after acceptance, before technical editing, formatting and proof reading. Using this free service, authors can make their results available to the community, in citable form, before we publish the edited article. This *Accepted Manuscript* will be replaced by the edited, formatted and paginated article as soon as this is available.

You can find more information about *Accepted Manuscripts* in the [Information for Authors](#).

Please note that technical editing may introduce minor changes to the text and/or graphics, which may alter content. The journal's standard [Terms & Conditions](#) and the [Ethical guidelines](#) still apply. In no event shall the Royal Society of Chemistry be held responsible for any errors or omissions in this *Accepted Manuscript* or any consequences arising from the use of any information it contains.

# Effect of selective oxidation of bacterial cellulose on degradability in phosphate buffer solution and their affinity for epidermal cell attachment

Xiangning Shi,<sup>a</sup> Qiuyan Cui,<sup>a</sup> Yudong Zheng,<sup>\*a</sup> Shuai Peng,<sup>a</sup> Guojie Wang,<sup>a</sup> Yajie Xie<sup>a</sup>

Corresponding author: zhengyudong@mater.ustb.edu.cn

<sup>a</sup>School of Materials Science and Engineering, University of Science and Technology Beijing, Beijing

100083, PR China

## Abstract

Bacterial cellulose (BC) has a very promising application in biomedical engineering due to its three dimensional nano-network and good biocompatibility. However, it is difficult for BC to degrade in vivo without cellulase, which has limited its potential application. In this work, oxidized bacterial cellulose (OBC) was prepared according to selective oxidation with NO<sub>2</sub> gas. The structure and micromorphology of OBC were characterized by FTIR, XRD, and SEM respectively. The results showed that the oxidation did not break the crystal structure and the crystallinity of BC. OBC still kept the 3D nano-fibrils network, while the diameter of each fiber in the nano-fibrils network of OBC became wider. When immersed in PBS, OBC degraded gradually. The mass loss rate and degradation rate of OBC were much higher than those of BC after degradation for 60 days. Degradation occurred from surface to inside and the oxidized part of the network favored the process. Results of cell-adhesion and proliferation studies also revealed that OBC had excellent cellular affinity as that of BC.

**Keywords:** Bacterial Cellulose, Oxidization, Degradability, cellular affinity

## 1. Introduction

As a polymeric material with nanofiber-network structure, BC has various perfect properties such as high water holding capacity, high crystallinity, high tensile

\* Corresponding Author: YD Zheng (Email: zhengyudong@mater.ustb.edu.cn, Tel: 86-10-62330802)

27 strength, good biocompatibility as well as in situ moldability and low production cost  
28 <sup>1-3</sup>, which has made it to be one of the most promising tissue engineering scaffold  
29 materials. At present, BC has a good application in wound covering, brain membrane,  
30 skin of tissue engineering, renovating artificial blood vessels and cornea etc <sup>4-6</sup>.  
31 However, the degradability of BC in human body has become one of the key factors  
32 that constrain its potential application in tissue engineering, since there is no cellulase  
33 in body fluids.

34 Oxidization of cellulose is an effective method to modify the chemical structure in  
35 order to improve its degradability in vivo for biomedical applications <sup>7</sup>. Cellulose has  
36 already been oxidized by different oxidant such as TEMPO-NaClO-NaBr <sup>8-10</sup>, NaIO<sub>4</sub>  
37 <sup>11, 12</sup>, NO<sub>2</sub> <sup>13, 14</sup>, HNO<sub>3</sub>/H<sub>3</sub>PO<sub>4</sub>/NaNO<sub>2</sub> <sup>15</sup> through which the primary alcohol groups at  
38 C6 were selectively oxidized into carboxyl during these oxidation process. Oxidized  
39 cellulose can be used as Surgicel to stop bleeding <sup>16</sup>. Besides, the oral adsorbent which  
40 is gotten from 2, 3-dialdehyde cellulose compounds can also function well in treating  
41 Chronic Renal Failure <sup>17</sup>. Recently, 2, 3-dialdehyde bacterial cellulose (DABC)  
42 oxidized by periodate was prepared <sup>18</sup>, which made its degradation rate in PBS was  
43 faster than that of BC, but the crystallinity and mechanical strength were much lower.  
44 Nitrogen dioxide (NO<sub>2</sub>) with excellent selectivity is considered as a more suitable  
45 oxidant for cellulose <sup>19</sup> among the oxidants as secondary reactions were almost  
46 avoided. We have used NO<sub>2</sub> to oxidize bacterial cellulose in gaseous environment for  
47 different time and got OBC with carboxyl groups at C6 <sup>20</sup>. The oxidation did not  
48 affect the crystal structure of BC, but changed the morphology of its network with  
49 wider diameter. Results showed that the oxidation reaction was controllable for  
50 regulating the degree of degradation of BC. However, structural changes, aggregative  
51 state during degradation, and cellular affinity of OBC have not been studied yet.  
52 Besides, degradation rate of OBC according to glucose concentration in PBS was not  
53 detected either.

54 In this work, we focused on further discussing and analyzing the degradation of  
55 oxidized bacterial cellulose. The degradation performance in vitro including changes  
56 in degradation rate, chemical and crystal structural and micromorphology changes of

57 OBC and BC were characterized and compared. Simultaneously, degradability of  
58 OBC was analyzed and degradation mechanism was then proposed. The cellular  
59 affinity of OBC was also evaluated and compared with that of BC.

## 60 **2. Experiments**

### 61 *2.1. Preparation of OBC*

62 Hainan Yida Food Co, Ltd supplied the BC membranes. As a pre-treatment, BC  
63 membranes were immersed in 10% NaOH solution for 30min at 80°C to remove the  
64 bacterial cell debris, then thoroughly washed to neutral by de-ionized water. NO<sub>2</sub> was  
65 produced by adding a suitable amount of Cu to superfluous HNO<sub>3</sub> (65 wt %) solution.  
66 NO<sub>2</sub> reacted with purified BC (15 mm in diameter and 1 mm in thickness) for 3, 6, 9  
67 and 12 days following the method last used.

### 68 *2.2 Degradability in vitro*

69 Degradation of BC and OBC was tested *in vitro* in phosphate buffered saline  
70 solution (PBS, PH=7.4) at 37°C. Films of BC and OBC were cut into circular slices  
71 with a diameter of 15mm, and then immersed in PBS in centrifuge tubes. The samples  
72 were taken out and washed by de-ionized water separately after degradation for 3, 6, 9,  
73 12, 15, 18, 21, 24, and 30 days, then freeze-dried and weighed. The original mass of  
74 each sample was designated as  $m_0$  while the mass after degradation was characterized  
75 as  $m_1$ . Mass loss rate is the ratio of reduced mass and original mass, which was  
76 calculated by the Equation (1).

77 Ultraviolet spectrophotometer (Unico, UV-2100) was used to test the glucose  
78 content as degradation product. Its absorbency at 470 nm has a liner relationship with  
79 the concentration of glucose solution. Degradation rate is the ratio of actual glucose  
80 mass and original mass which was measured to analyze degradation degree of OBC.  
81 Concentration of glucose was noted as C and volume of degradation solution was  
82 designed as V. Degradation rate were calculated by the Equation (2)<sup>21</sup>.

$$83 \quad \text{Mass loss} = \frac{m_1 - m_0}{m_0} \times 100\% \quad (1)$$

84 
$$\text{Degradation rate} = \frac{C \times V}{m_0} \times 100\% \quad (2)$$

85 Special software Spss 13 was also used to statistically analyze the data of mass  
86 loss and concentration of glucose related to degradation rate. The data between three  
87 groups were analyzed with variance. All data were represented by average  $\pm$  standard  
88 deviation ( $\bar{x} \pm \text{sd}$ ).

### 89 *2.3 Cellular affinity test*

90 Three groups of materials (named group a: blank control, group b: OBC, group c:  
91 BC) were cut into discs with a diameter of 15 mm and heat-sealed after package with  
92 plastic zip-lock bags. Samples were then sterilized under 18.40kGy with radiation of  
93 Co60. Experiments of cell cultivation were performed in compliance with the relevant  
94 laws and institutional guidelines and approved by No. 1 Hospital affiliated to General  
95 Hospital of the Chinese People's Liberation Army.

96 Newborn fetal rat was executed and immersed in 75% ethanol for 3 min. After  
97 that, subsequent operations were all under aseptic conditions. Torso skin was sheared  
98 off from the body of the rat. Then torso skin was cut into pieces of 0.5 cm<sup>2</sup> and  
99 immersed in a mixture solution of 0.25% trypsin and 0.02% EDTA for 16h at 4°C in  
100 refrigerator. Then epidermic was removed from the dermis and put into centrifugal  
101 tube containing dulbecco's modified eagle medium (DMEM). Epidermal cells formed  
102 cell suspension due to blowing with straw. The original number of epidermal cells  
103 was microscopically counted and centrifugation treatment at the speed of 1000 r/min  
104 for 5min was followed subsequently. DMEM solution containing 10% tire bovine  
105 serum was added to the suspension, adjusting the density of cells into  $1 \times 10^4$  /mL. The  
106 suspension was then inoculated in 24-hole training board coated with 1 ml mouse-tail  
107 collagen per hole in advance.

108 Three groups of materials were placed in holes respectively after suspension's  
109 sedimentation for 1 h. They were then incubated in hatch box under the condition of  
110 5% CO<sub>2</sub> at 37°C. Culture solution was renewed at the time of 4 and 7 days

111 respectively. After 1, 4, 7, 10 days, cells cultivated with different materials were taken  
112 out and observed under optical microscope, then the cell numbers were  
113 microscopically counted and cell viability was tested through MTT method.

#### 114 *2.4. Characterization*

115 The microstructure of BC and OBC was observed by scanning electron  
116 microscopy (SEM, Apollo 300, and 10 KV). All of the samples were freeze-dried and  
117 coated with a thin layer of gold in a sputter coater in advance.

118 Chemical structure of BC and OBC before and after degradation for different  
119 time was tested by Fourier Transform Infrared Spectroscopy (FTIR, NICOLET 750)  
120 with a range of frequency from  $4000\text{ cm}^{-1}$  to  $450\text{ cm}^{-1}$  and a resolution of  $4\text{ cm}^{-1}$ .

121 X-ray diffractometry (XRD, D/MAX-RB, 20 kV, 40 mA) with Cu  $\alpha$  radiation  
122 ( $\lambda=0.154\text{nm}$ ) was used to examine the crystal structure of the samples. The range of  
123 diffraction angles ( $2\theta$ ) was  $10^\circ$ - $40^\circ$ .

### 124 **3. Results and Discussion**

#### 125 *3.1 Mass loss and degradation rate*

126 The mass loss rate and degradation rate are often used to assess the degradation  
127 of biomaterials in vitro <sup>22</sup>. When immersed in PBS, both BC and OBC began to  
128 degrade from surface in, degraded debris and fragments dropped from original films  
129 of BC and OBC, leading to mass loss of original materials. The degradation product  
130 of cellulose is glucose, so as for oxidized cellulose. Therefore, glucose content  
131 represents their biodegradability in a way. Standard curve of glucose concentration  
132 showed the content match the absorbance at 470 nm wavelength in linear relationship  
133 well. The glucose concentrations of different degradation stage were measured  
134 accurately, and the degradation rates were calculated according to Equation (2).

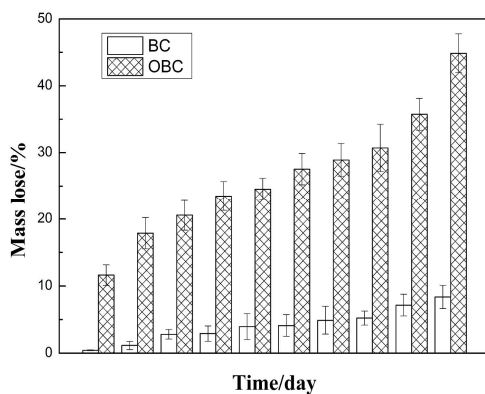


Fig.1 Mass loss rate of BC and OBC

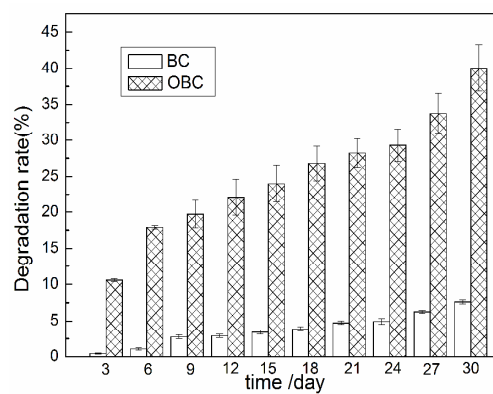


Fig.2 Degradation rate of BC and OBC

135

136

137

138

139

140

141

142

143

144

145

146

147

148

149

150

151

152

153

154

155

156

157

158

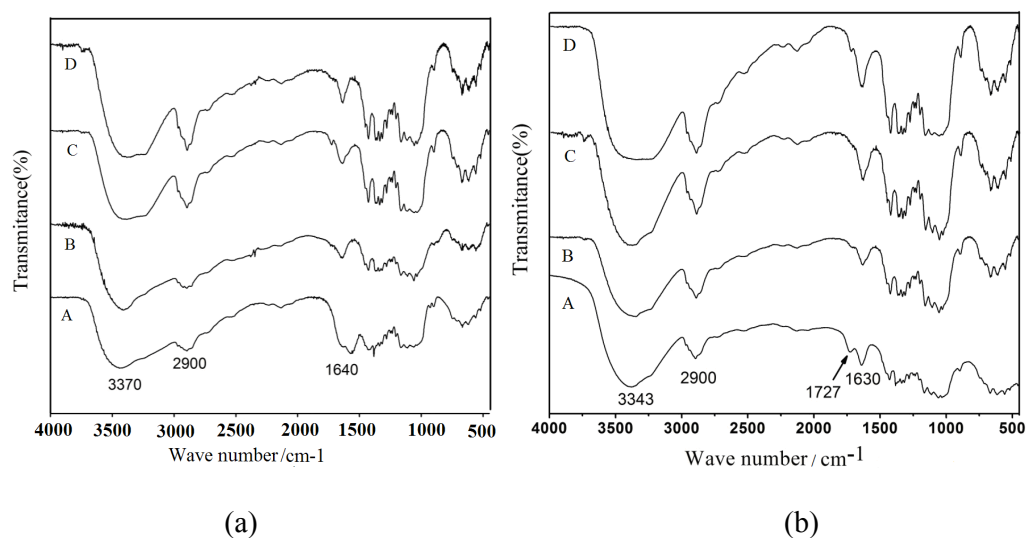
Fig. 1 shows the mass loss of BC and OBC. Just as expected, the mass loss rate of OBC was much higher than that of BC obviously. For BC, the mass loss rate was less than 10% (wt) even after 60 days in PBS solution (Fig.1), which was in consistence with the results reported by Peng<sup>20</sup> and Li<sup>18</sup>. For OBC, however, it even rose up to 45% as time extends. For DABC as reported by Li<sup>18</sup>, the mass loss rate was about 80% after 1000h (about 41.5 days). Apparently, the mass loss rate of OBC in Fig.1 was lower than that of 2, 3-dialdehyde bacterial cellulose (DABC), this is mainly because oxidation by NO<sub>2</sub> is much milder<sup>19</sup> than that of periodate and degradation accompanied with oxidation was slight. Moreover, OBC with 45% mass loss after degradation *in vitro* for 60 days still maintained its initial shape and partial mechanical properties, implying more or less that oxidation occurred in the BC membrane was a uniform selective one. Besides, the high crystalline degree and less crystal defects of OBC may also helped to interpret its slow degradation speed in comparison with electrospun plant cellulose oxidized by NO<sub>2</sub><sup>23</sup>.

The existence of glucose in PBS solution suggests that the C-O-C bond become weakened and cracked after degradation, which contributed to the production of small molecular of glucose as well as the degradation of BC and OBC. Degradation rate of BC and OBC (Fig.2) kept the same trend with mass loss rate as time passed. The degradation rate of BC was less than 8% after 60 days, while for OBC, it came up to 40% (Fig.2), indicating that degradation of OBC in PBS solution was greatly sped up and OBC was easier to degrade in PBS solution with its characteristic carboxyl groups at C6 due to the selective oxidization.

159 Another significant phenomenon is that during early times of degradation, the  
 160 mass loss rate was always higher than degradation rate for BC as well as for OBC.  
 161 This is because mass loss was calculated according mass before and after degradation,  
 162 while degradation rate was achieved through glucose concentration in PBS. When  
 163 materials began to degrade, small fragments such as fiber bundles left materials,  
 164 causing mass loss. However, these bundles do not decomposed into glucose  
 165 completely at once, leading to relatively lower degradation rate than mass loss rate.  
 166 Overall, there is no big difference between mass loss and degradation rate, since most  
 167 of the fiber bundles finally degraded into glucose after falling off. Therefore, we are  
 168 sure that BC and OBC have degraded in PBS solution and OBC possess a higher  
 169 degradation rate.

### 170 3.2 Structural changes of BC and OBC after degradation

171 The hydroxyl groups at the position C6 of cellulose could convert to carboxyl  
 172 groups when selectively oxidized by  $\text{NO}_2$ . Fig.3 shows the chemical structure of OBC  
 173 together with BC before and after degradation for different time.



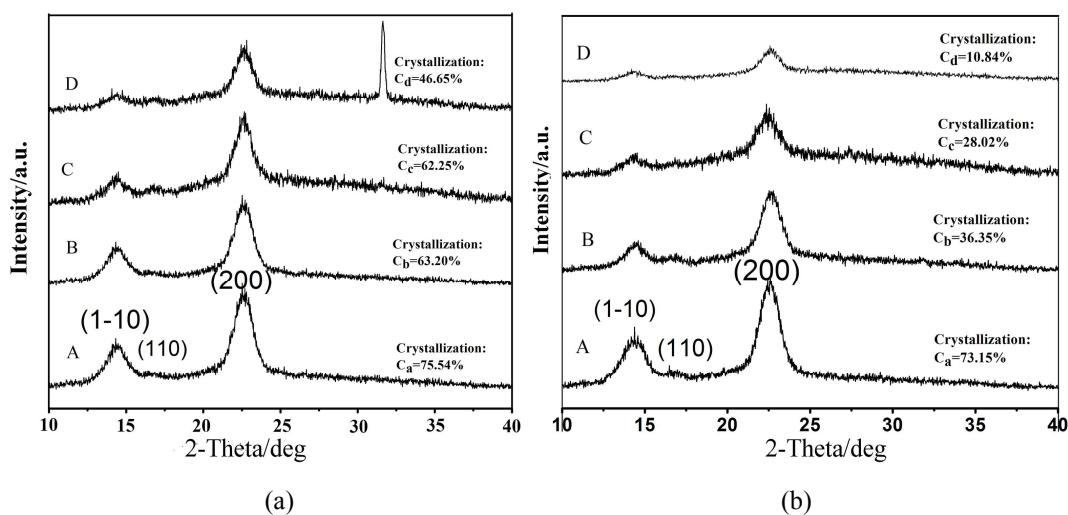
176 Fig.3 FTIR spectra of (a)BC and (b)OBC degraded in PBS respectively for (A) 0 day, (B) 12 days,  
 177 (C) 30 days, (D) 60 days.

178 For original BC, there are three absorption peaks at 3370, 2900, and 1060  $\text{cm}^{-1}$   
 179 corresponding to the stretching vibrations of the group  $\nu(-\text{OH})$ ,  $\nu(-\text{CH}_2)$  and  $\nu$



180 (C-O) respectively <sup>24,25</sup> (Fig.3a curve A). Compared with FTIR curve of original BC,  
 181 new absorption peaks appeared at  $1727\text{cm}^{-1}$  assigned as C=O stretching vibration of  
 182 carboxyl groups after oxidation, indicating the existence of the oxidation product —  
 183 carboxyl cellulose. Meanwhile, the intensity of absorption peaks near  $1320\text{-}1210\text{ cm}^{-1}$   
 184 associated with the C-O groups decreased obviously, further proving the formation of  
 185 OBC (Fig.3b curve A). After degradation in PBS for different time, the peaks of  
 186 hydroxyl groups of BC were all obviously strengthened (Fig.3a curve B, C, D and  
 187 Fig.3b curve B, C, D), while the typically characteristic peak of OBC appeared at  
 188  $1727\text{cm}^{-1}$  corresponding to C=O stretching vibration disappeared (Fig.4b curve D).  
 189 That means more hydroxyl groups formed due to the broken of C-O-C bond and  
 190 degradation occurred at the position of C6.

### 191 3.3 Crystal structure comparison of BC and OBC after degradation



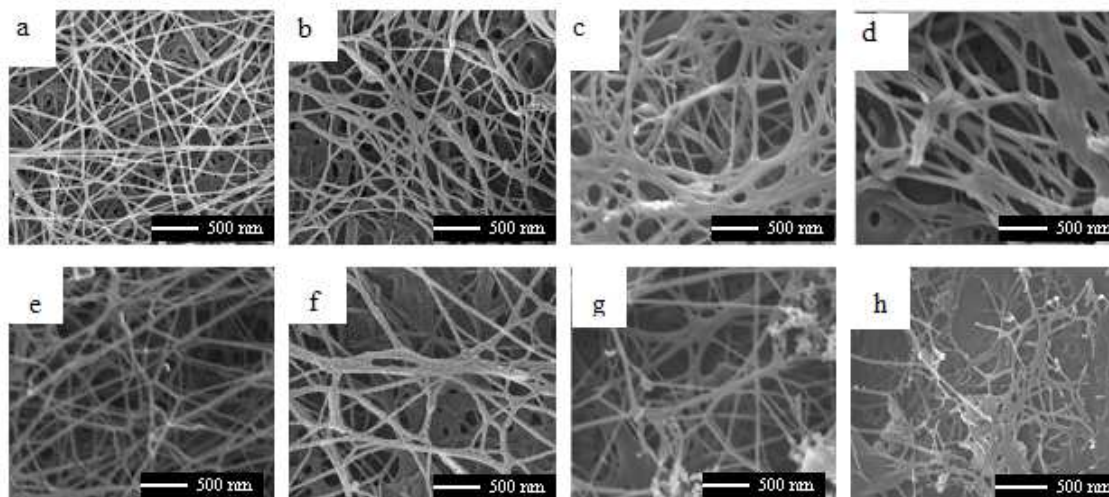
192  
 193 (a) (b)  
 194 Fig.4. XRD patterns of (a)BC and (b)OBC immersed in PBS for (A)0 day, (B)12 day, (C)30 days,  
 195 (D)60 days.

196 Fig.4 shows the XRD patterns of BC and OBC degraded for different times. For  
 197 original BC (Fig.4a curve A), three peaks are located at diffraction angles of  
 198  $14.6^\circ, 16.5^\circ$  and  $22.5^\circ$  respectively corresponding to the primary diffraction of the  
 199 crystal plane (1-10), (110) and (200), which shows the structure of well-defined  
 200 cellulose I crystal <sup>26-29</sup>. The diffraction peaks of OBC according to Fig.4b curve A are  
 201 almost the same as those of original BC, implying that OBC still retained the crystal

202 structure of cellulose I and the oxidation had little impact on the crystal structure as  
203 well as their crystallinity<sup>30</sup>.

204 When immersed in PBS solution for different time, crystallinity of both BC and  
205 OBC decreased, the crystallinity of BC decreases from 75.54% to 46.65% as time  
206 extends from 0 day to 60 days (Fig.4a), while for OBC, it ranged from 73.15% to  
207 10.84% (Fig.4b). This is because with the presence of carboxyl groups and higher  
208 activity, a long-term degradation of OBC enabled water molecules to permeate into  
209 inner crystalline regions, leads to a loose arrangement of molecular chains and  
210 expanded amorphous regions<sup>31, 32</sup>. At the same time, degradation in amorphous  
211 regions was under way and all above helps to drop crystallinity down. Besides, the  
212 intensity of diffraction peaks mentioned above weakened as time passed, especially  
213 for OBC. Peaks at crystal plane (1-10) of OBC nearly disappeared after immersion for  
214 30 days and 60days (Fig.4b curve D). Obviously, crystallinity of OBC decreased more  
215 sharply compared with BC, indicating that OBC was much easier to degrade in PBS  
216 solution because of the active action of carboxyl groups at C6 position. The similar  
217 phenomenon was also reported by Li<sup>18</sup> and Calvini<sup>33</sup>.

### 218 3.4 Surface morphology



219

220

221 Fig.5. SEM of BC and OBC before (a, b, c, d) and after (e, f, g, h, corresponding to a, b, c, d  
222 respectively) degradation for 60days (a)BC, (b) OBC oxidized for 3 days, (c) 6 days, (d) 12 days.

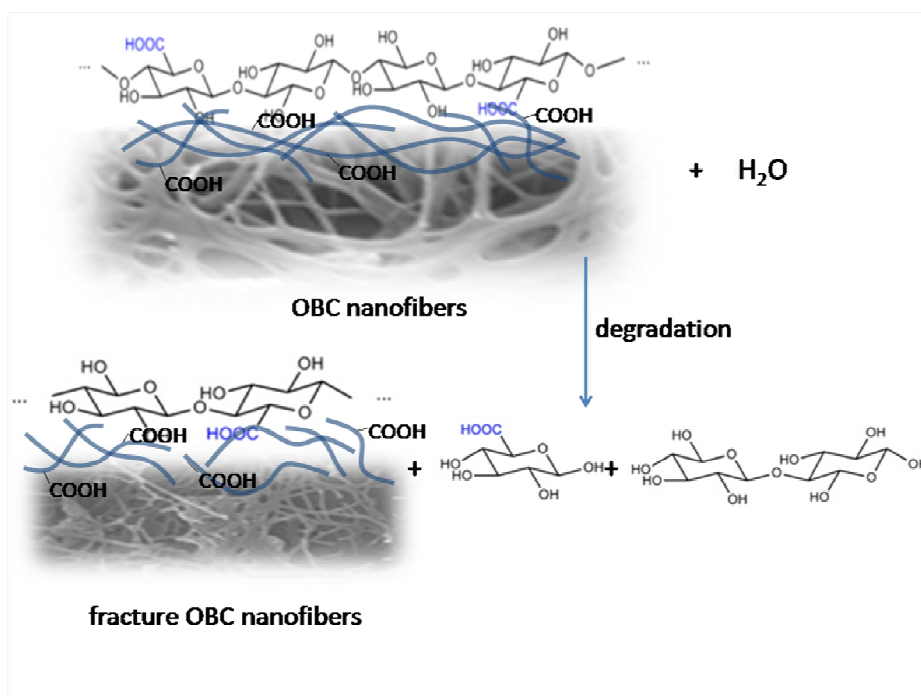
223 Fig.5 showed the SEM images of BC and OBC before and after degradation for  
224 60 days. BC had a dense 3-dimension network structure of the nanofibrils, which was  
225 almost retained after oxidation. Meanwhile, the nanofibrils of OBC appeared to  
226 aggregate or fuse into bundles gradually after oxidization for different time (Fig.5b, c,  
227 d). In addition, a few fibrils began to be fragmented by the oxidation process  
228 (Fig.5d). That is to say, oxidation was accompanied by a light degree of deterioration  
229 visible on oxidized fibers, which was similar to the phenomenon described by Kim<sup>15</sup>  
230 and Kumar<sup>34</sup>.

231 After degradation in PBS solution for 60 days, BC maintained the original  
232 nano-fibrous networks with a few fibrils ruptured (Fig.5e). While for OBC oxidized  
233 for 3 days, more fibrils ruptured and its network became loose (Fig.5f). The 3D  
234 nano-fibrous network of OBC oxidized for 6 days partly disappeared, and many  
235 fibrils fracture and fell into pieces (Fig.5g) because of the accelerated degradation of  
236 OBC. More OBC fibers eroded and the nano-fibrous network was almost collapsed  
237 after degradation for 60 days for OBC oxidized for 12 days (Fig.5h), which was in  
238 consistent with its high mass loss rate and degradation rate of 40% above. Obviously,  
239 the oxidization of BC by NO<sub>2</sub> sped up the degradation of OBC, which could gradually  
240 destruct nano-fibrous network of OBC at a desirable degradation rate by controlling  
241 time.

### 242 *3.5 Discussion and analysis on degradation mechanism*

243 It is well known that BC degrades very slowly without cellulase, however,  
244 oxidization can help to improve its degradability, which has been proved by results  
245 above. When immersed in PBS, both BC and OBC would illimitably swell from  
246 surface in, and the crystallinity and the binding force of hydrogen bonds within and  
247 between molecular chains would decline<sup>35</sup>, leading to the fracture of hydrogen bonds  
248 at the position of C2, C3 and C6, which could induce the formation of new hydrogen  
249 bonds with water molecule. For both BC and OBC, swelling first began from  
250 amorphous regions and surface of crystalline regions during degradation. That is to  
251 say, degradation occurred from amorphous regions and surface of crystalline regions,

252 then moved to inner crystalline regions when increasing the time. Breakage of  
 253 structure turned from crystalline regions to amorphous ones, leading to the decrease  
 254 of crystallinity and causing the wideness and excursion of hydroxyl groups peaks  
 255 (Fig.3). This process contributed to the further swelling and degradation of cellulose  
 256 macromolecular chain as a long-term swelling enabled water molecules to permeate  
 257 into inner regions and turned it to be a looser arrangement of molecular chains with  
 258 expanded amorphous regions<sup>36</sup>. Then the bond C-O-C between monomers broke and  
 259 degraded parts dropped from surface, leading to mass loss. After that, the original  
 260 inner parts turned out to be surface and expose to PBS to repeat the process. This  
 261 regular pattern of degradation is in line with that of 2, 3-dialdehyde bacterial cellulose  
 262 reported by Kim<sup>12</sup> and Calvini<sup>33</sup>.



263

264

Fig.6 Degradation and breaking of OBC molecule chains

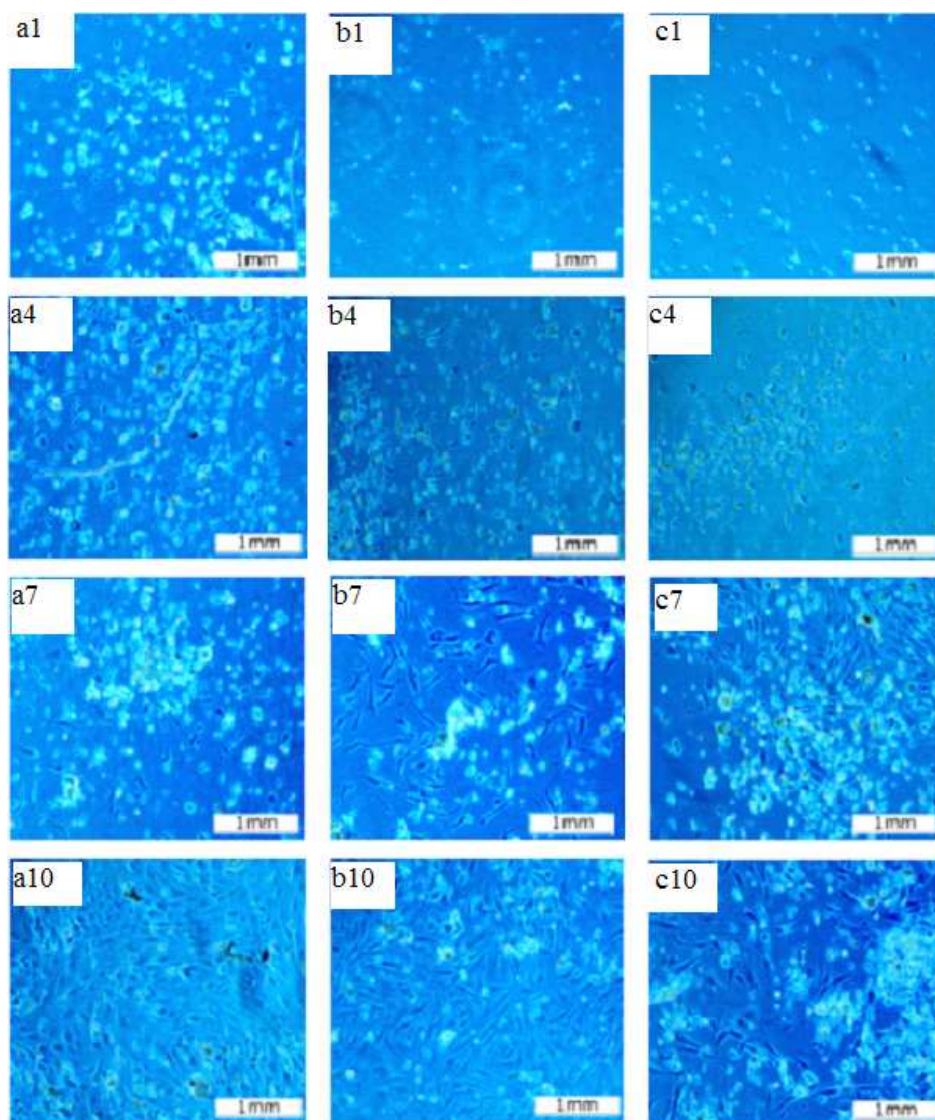
265 What made OBC degrade faster than BC is that after oxidation, carboxyl groups  
 266 of OBC at C6 possess higher energy as well as better activity. Meanwhile carboxyl  
 267 groups are easier to rotate around bond of C5-C6 than hydroxyl group, which makes  
 268 the bond between monomers of OBC more liable to fracture than BC. The  
 269 degradation process of OBC is shown in Fig.6. Molecule chains of OBC first break  
 270 into short chains with different degrees of polymerization, then these shorter chains

271 finally degraded into glucose. This phenomenon was close to the reported value for  
272 the periodate oxidation modified on BC<sup>20,33</sup>. Besides, OBC with better hydrophilia  
273 due to carboxyl group at C6 enables OBC to absorb more water molecules, which will  
274 also contribute to its hydrolysis. Furthermore, as mentioned in 3.3, the crystallinity of  
275 BC was 75.54% while the crystallinity of OBC was 73.15%. With the presence of  
276 carboxyl groups and higher activity, OBC enabled water molecules to permeate into  
277 inner crystalline regions, leads to a loose arrangement of molecular chains and  
278 expanded amorphous regions which caused a faster degradation. All above helps to  
279 drop crystallinity down. The disappearance of C=O peaks (Fig.4.b) proved that the  
280 molecular chains break into terminal groups at the position of carboxyl group when  
281 they degraded in PBS solution, which lead to reduce even complete vanishing of  
282 peaks of carboxyl groups.

283 Crystalline region contributes greatly to the strength of cellulose<sup>37</sup> and mechanical  
284 properties of cellulose often deteriorated by secondary oxidation process<sup>25</sup>. Therefore,  
285 it is necessary to investigate the mechanical properties and other physical properties  
286 of OBC oxidized by NO<sub>2</sub>, which is an ongoing study.

### 287 *3.6 Cells cultivation*

288 Direct culture method was adopted to evaluate and compare the cellular affinity  
289 of OBC with BC. The epidermal cells of fetal rat were co-cultivated with three groups  
290 of materials (a: blank control, b: OBC and c: BC) for different time. After seeding  
291 epidermal cells on these samples, the cell proliferations status and cytomorphology  
292 after cultivation for 1, 4, 7, and 10 days are shown in Fig.8, respectively.



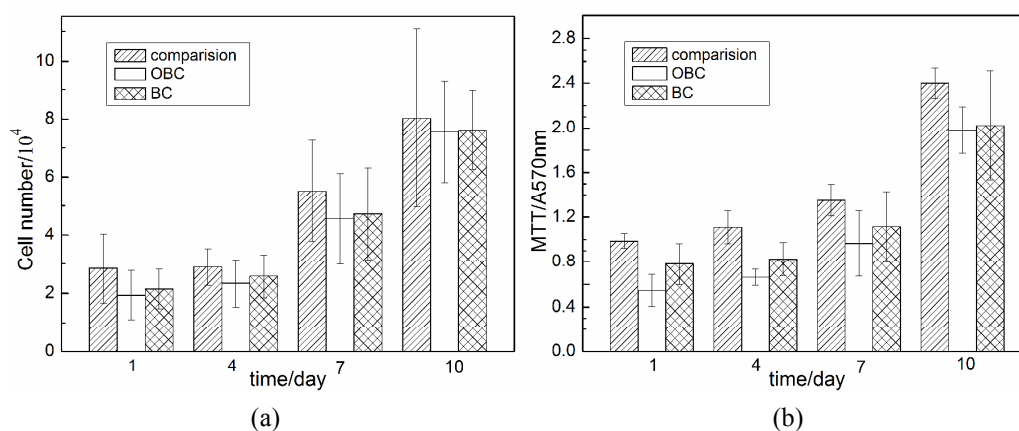
293

294 Fig.7 Optical photos of proliferation status (cytomorphology) of epidermal cells after cultivation  
295 with different samples (a: blank control, b: OBC and c: BC): a1, b1 and c1 for 1 day; a4, b4 and c4  
296 for 4 days; a7, b7 and c7 for 7 days; a10, b10 and c10 for 10 days.

297 Obviously, non-transparent small cells with an orbicular shape observed under  
298 optical microscope are epidermal cells while others are fibroblast ones. On the whole,  
299 cells amount rose continuously as time extended. As cultivated for 1day, a small  
300 number of cells distributed in DMEM solution dispersedly (Fig.7). The cells number  
301 of group was more than that of group b and group c. After 4 days, more colonies of  
302 epidermal cells in three groups appeared together with several fibroblast cells. Cells  
303 gathered and overlapped mutually. Cells on the edge grew outside with a form of

304 single layer, contributing to the extension of colonies (Fig.7). Orbicular epidermal  
 305 cells and spindly fibroblasts proliferated rapidly when it came to 7 days. Epidermal  
 306 cells merged into small areas. At the same time, the missdistance among three groups  
 307 decreased. After 10 days, fibroblast cells proliferated abundantly, especially for group  
 308 a, in which fibroblast cells almost filled the whole area. For group b and group c,  
 309 more epidermal cells grew and their numbers increased apparently (Fig.7). The total  
 310 of epidermal cells and fibroblast ones in each group became almost the same finally,  
 311 suggesting that BC and OBC both support cell proliferation.

### 312 3.7 Cellular affinity evaluation



313  
 314

315 Fig.8 Cellular affinity of OBC compared with blank control and BC (a) epidermal cell numbers  
 316 during the proliferation, (b) MTT of cells cultivated with different materials.

317 Fig.8a shows specific number of epidermal cells during proliferation when  
 318 cultivated in vitro. Just the same as the results observed in Fig.8, epidermal cells  
 319 number grew slowly during early days and then became fast. The numbers of  
 320 epidermal cells cultivated with three groups of materials all slightly rose after one-day  
 321 proliferation and cells of group a is a little more than that of b and c. After 4 days,  
 322 epidermal cells numbers in three groups all increase slightly, in which group a is still  
 323 the most. When it comes to 7 days, epidermal cells proliferate faster than before and  
 324 differences among three groups minished ( $P < 0.05$ ). When cultivated for 10 days,  
 325 distinction among cells numbers of three groups almost significantly disappeared ( $P <$   
 326  $0.05$ ). On the whole, cell growth of three groups share the consistent trend without  
 327 great differences, suggesting that BC and OBC have little impact on cell proliferation

328 and they both support cell proliferation with good cellular affinity.

329       The MTT data describe the relative viability of cells including epidermal cells as  
330 well as fibroblast cells growing on the surface of different materials. The data are  
331 comparable since the same numbers of cells were added to samples. Consequence of  
332 MTT colorimetric estimation is shown in Fig.9b. MTT values of group a kept the  
333 most all along the cultivation. MTT values of cells cultivated for 4 day were almost  
334 the same with that of cells cultivated for 1day. When 7 days passed, data increased a  
335 little. While for 10 days, MTT values rose up to a high level resulted from the  
336 proliferation of both epidermal cells and fibroblast cells. These materials hardly affect  
337 proliferation of epidermal cells. As result of MTT colorimetric estimation is in line  
338 with cell growth number to same extent, we can arrive at the conclusion that OBC and  
339 BC support cell proliferation with good biocompatibility, which extends their  
340 potential application in vivo as implanted materials.

#### 341 **4. Conclusions**

342       OBC oxidized by NO<sub>2</sub> in aphotic condition keeps the original 3D nano-fibrous  
343 network crystal structure of BC with relatively wider diameter and it is prone to  
344 degrade in PBS solution more easily according to mass loss and degradation rate  
345 compared with BC. For OBC, the mass loss rate went up to 45% after 60 days while it  
346 was only approximately 10% for BC. FTIR spectra of OBC immersed in PBS for  
347 different time also suggest that the degradation procedure of OBC first occurs from  
348 amorphous regions and surface of crystalline regions, then moves to inner crystalline  
349 regions. Carboxyl groups with higher energy and better activity are easier to rotate  
350 around bond of C5-C6 than hydroxyl group, help the bond between monomers of  
351 OBC more liable to break than BC. Oxidation has little effect on the crystal structure  
352 of bacterial cellulose. After degraded in PBS solution, Crystallinity of OBC decreases  
353 sharply, indicating that OBC is much easier to degrade in PBS solution and further  
354 proved the degradation mechanism. According to SEM micrographs, OBC oxidized  
355 for different time degraded at varying degrees with fibrils fragmented more or less.  
356 When cultivated with epidermal cells of fetal rat, OBC showed a good cellular affinity,



357 contributing to a wider application in tissue engineering. Consequently, the selective  
358 oxidation by nitrogen dioxide has been proven to be a practicable method for  
359 modification of BC's degradability without weakening its biocompatibility and crystal  
360 structure.

361 *<sup>a</sup>School of Materials Science and Engineering, University of Science and Technology*  
362 *Beijing, Beijing, PR China*

363 E-mail: zhengyudong@mater.ustb.edu.cn. Fax:+86-010-62332336; Tel: +86-010-  
364 62330802

### 365 **Acknowledgements**

366 This study is financially supported by National Natural Science Foundation of  
367 China Project (Grant No.51273021, 51473019).

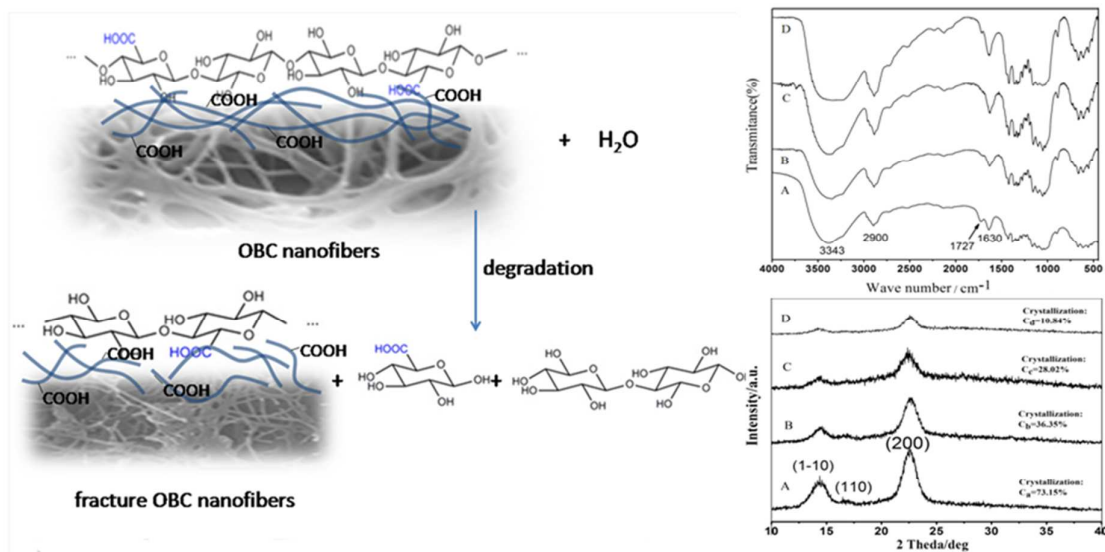
### 368 **References**

- 369 1. A. Svensson, E. Nicklasson, T. Harrah, B. Panilaitis, D. Kaplan, M.  
370 Brittberg and P. Gatenholm, *Biomaterials*, 2005, 26, 419-431.
- 371 2. K. Watanabe, Y. Eto, S. Takano, S. Nakamori, H. Shibai and S.  
372 Yamanaka, *Cytotechnology*, 1993, 13, 107-114.
- 373 3. G. Helenius, H. Bäckdahl, A. Bodin, U. Nannmark, P. Gatenholm  
374 and B. Risberg, *Journal of Biomedical Materials Research Part A*, 2006, 76,  
375 431-438.
- 376 4. W. Czaja, A. Krystynowicz, S. Bielecki and R. M. Brown Jr,  
377 *Biomaterials*, 2006, 27, 145-151.
- 378 5. H. Fink, J. Hong, K. Drotz, B. Risberg, J. Sanchez and A. Sellborn,  
379 *Journal of Biomedical Materials Research Part A*, 2011, 97, 52-58.
- 380 6. D. Klemm, D. Schumann, U. Udhardt and S. Marsch, *Progress in*  
381 *polymer science*, 2001, 26, 1561-1603.
- 382 7. R. L. Stilwell, M. G. Marks, L. Saferstein and D. M. Wiseman,  
383 *Handbook of biodegradable polymers*, 1998, 7, 291-306.
- 384 8. T. Saito, S. Kimura, Y. Nishiyama and A. Isogai,  
385 *Biomacromolecules*, 2007, 8, 2485-2491.
- 386 9. A. Isogai, T. Saito and H. Fukuzumi, *Nanoscale*, 2011, 3, 71-85.
- 387 10. Y. Kato, J. Kaminaga, R. Matsuo and A. Isogai, *Carbohydrate*  
388 *Polymers*, 2004, 58, 421-426.
- 389 11. A. Varma and M. Kulkarni, *Polymer Degradation and Stability*,  
390 2002, 77, 25-27.
- 391 12. U. J. Kim, S. Kuga, M. Wada, T. Okano and T. Kondo,

- 392 *Biomacromolecules*, 2000, 1, 488-492.
- 393 13. S. Coseri, G. Nistor, L. Fras, S. Strnad, V. Harabagiu and B.
- 394 Simionescu, *Biomacromolecules*, 2009, 10, 2294-2299.
- 395 14. L. Saferstein and G. Serafica, Google Patents, 2010.
- 396 15. C.-W. Kim, D.-S. Kim, S. Y. Kang, M. Marquez and Y. L. Joo,
- 397 *Polymer*, 2006, 47, 5097-5107.
- 398 16. M. C. Henry, D. B. Tashjian, H. Kasowski, C. Duncan and R. L.
- 399 Moss, *Journal of pediatric surgery*, 2005, 40, 9-11.
- 400 17. M. Yagi, S. Kato, T. Nishitoba, H. Sato, N. Kobayashi, N. Iinuma
- 401 and N. Nagano, *Nephron*, 1998, 78, 433-439.
- 402 18. J. Li, Y. Wan, L. Li, H. Liang and J. Wang, *Materials Science and*
- 403 *Engineering: C*, 2009, 29, 1635-1642.
- 404 19. S. Camy, S. Montanari, A. Rattaz, M. Vignon and J.-S. Condoret,
- 405 *The Journal of Supercritical Fluids*, 2009, 51, 188-196.
- 406 20. S. Peng, Y. Zheng, J. Wu, Y. Wu, Y. Ma, W. Song and T. Xi,
- 407 *Polymer bulletin*, 2012, 68, 415-423.
- 408 21. Y. Chen, T. Xi, Y. Zheng, T. Guo, J. Hou, Y. Wan and C. Gao,
- 409 *Journal of Bioactive and Compatible Polymers*, 2009, 24, 137-145.
- 410 22. A. Oyane, H. M. Kim, T. Furuya, T. Kokubo, T. Miyazaki and T.
- 411 Nakamura, *Journal of Biomedical Materials Research Part A*, 2003, 65,
- 412 188-195.
- 413 23. M. S. Khil, H. Y. Kim, Y. S. Kang, H. J. Bang, D. R. Lee and J. K.
- 414 Doo, *Macromolecular Research*, 2005, 13, 62-67.
- 415 24. Y. Maréchal and H. Chanzy, *Journal of molecular structure*, 2000,
- 416 523, 183-196.
- 417 25. M. Kačuráková, A. C. Smith, M. J. Gidley and R. H. Wilson,
- 418 *Carbohydrate Research*, 2002, 337, 1145-1153.
- 419 26. V. Klechkovskaya, Y. G. Baklagina, N. Stepina, A. Khripunov, P.
- 420 Buffat, E. Suvorova, I. Zhanaveskina, A. Tkachenko and S. Gladchenko,
- 421 *Crystallography Reports*, 2003, 48, 755-762.
- 422 27. C. Rambo, D. Recouvreux, C. Carminatti, A. Pitlovanciv, R.
- 423 Antônio and L. Porto, *Materials Science and Engineering: C*, 2008, 28,
- 424 549-554.
- 425 28. L. Yu, J. Lin, F. Tian, X. Li, F. Bian and J. Wang, *Journal of*
- 426 *Materials Chemistry A*, 2014, 2, 6402-6411.
- 427 29. J. Lin, L. Yu, F. Tian, N. Zhao, X. Li, F. Bian and J. Wang,
- 428 *Carbohydrate polymers*, 2014, 109, 35-43.
- 429 30. V. Chavan, B. Sarwade and A. Varma, *Carbohydrate polymers*,
- 430 2002, 50, 41-45.
- 431 31. M. H. Lee, H. S. Park, K. J. Yoon and P. J. Hauser, *Textile Research*
- 432 *Journal*, 2004, 74, 146-154.
- 433 32. L. Hong, Y. Wang, S. Jia, Y. Huang, C. Gao and Y. Wan, *Materials*

- 434 *Letters*, 2006, 60, 1710-1713.
- 435 33. P. Calvini, A. Gorassini, G. Luciano and E. Franceschi, *Vibrational*  
436 *spectroscopy*, 2006, 40, 177-183.
- 437 34. V. Kumar and Y. Tianrun, *Carbohydrate polymers*, 2002, 48,  
438 403-412.
- 439 35. W. Mormann and U. Michel, *Carbohydrate polymers*, 2002, 50,  
440 349-353.
- 441 36. H. Yamamoto and F. Horii, *Macromolecules*, 1993, 26, 1313-1317.
- 442 37. F. Goelzer, P. Faria-Tischer, J. Vitorino, M.-R. Sierakowski and C.  
443 Tischer, *Materials Science and Engineering: C*, 2009, 29, 546-551.
- 444
- 445

## Graphical abstract



The structure and micromorphology of oxidized bacterial cellulose (OBC) selective oxidized with  $\text{NO}_2$  gas were characterized. The mass loss rate and degradation rate of OBC were much higher than those of BC after degradation for 60 days. The oxidation did not break the crystal structure and the crystallinity of BC. OBC still kept the 3D nano-fibrils network, while the diameter of each fiber in the nano-fibrils network of OBC became wider. When immersed in PBS, OBC degraded gradually. Degradation occurred from surface to inside and the oxidized part of the network favored the process. Results of cell-adhesion and proliferation studies also revealed that OBC had excellent cellular affinity as that of BC.

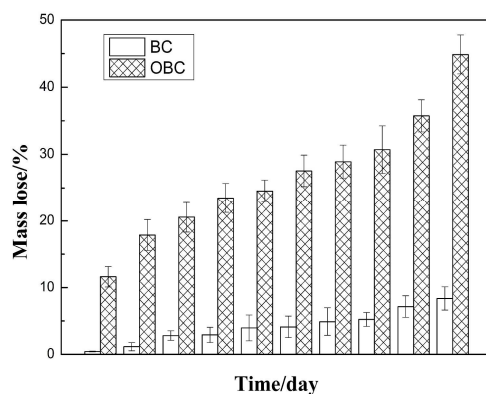
1           **Effect of selective oxidation of bacterial cellulose on**  
2           **degradability in phosphate buffer solution and their affinity**  
3           **for epidermal cell attachment**

4           Xiangning Shi,<sup>a</sup> Qiuyan Cui,<sup>a</sup> Yudong Zheng,<sup>\*a</sup> Shuai Peng,<sup>a</sup> Guojie Wang,<sup>a</sup> Yajie Xie<sup>a</sup>

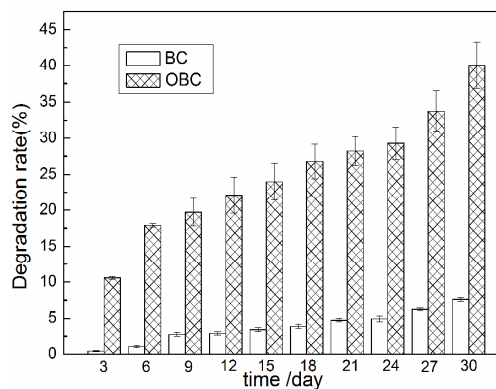
5           Corresponding author: zhengyudong@mater.ustb.edu.cn

6           <sup>a</sup>School of Materials Science and Engineering, University of Science and Technology Beijing, Beijing

7           100083, PR China

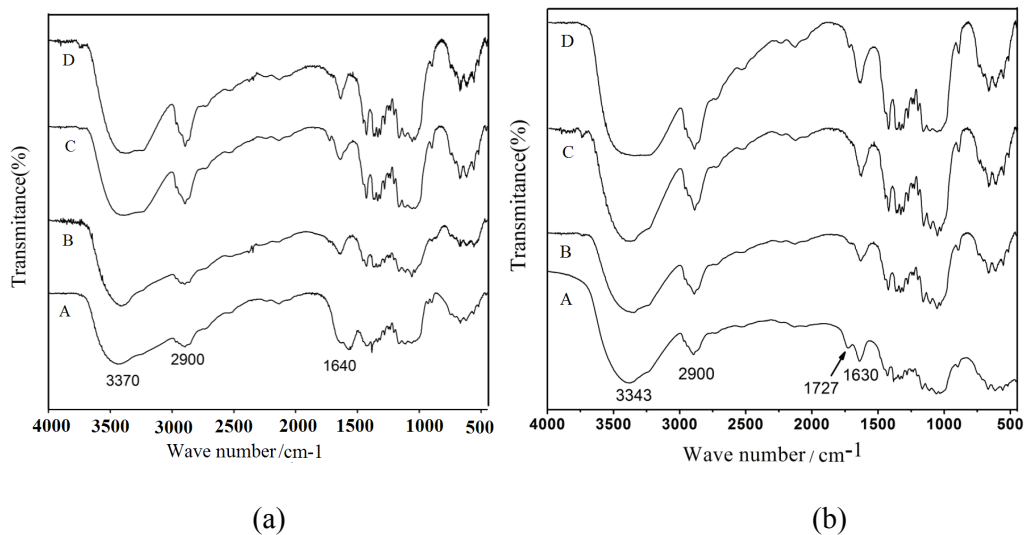


8           Fig.1 Mass loss rate of BC and OBC



9           Fig.2 Degradation rate of BC and OBC

10  
11           \* Corresponding Author: YD Zheng (Email: zhengyudong@mater.ustb.edu.cn, Tel: 86-10-62330802)



12

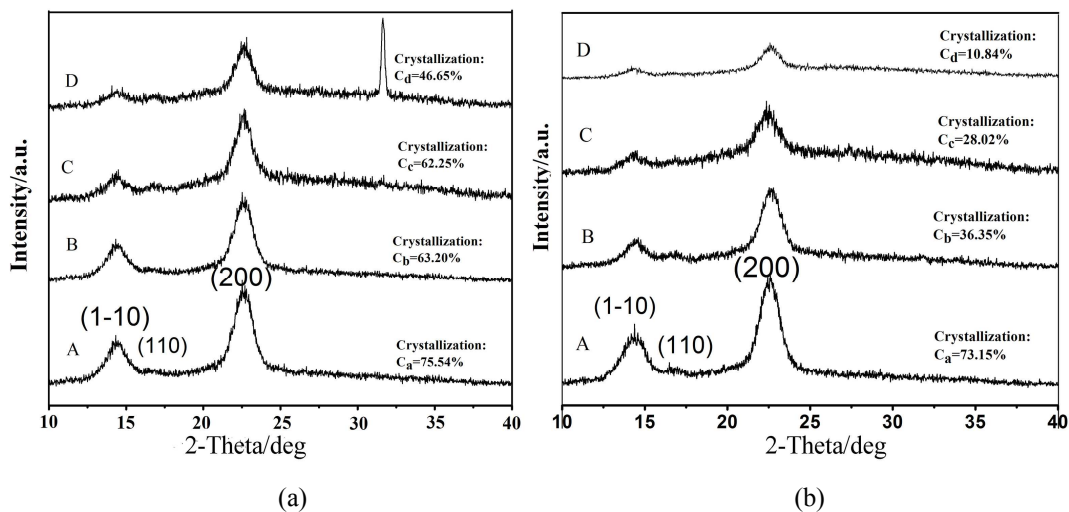
13

14 Fig.3 FTIR spectra of (a)BC and (b)OBC degraded in PBS respectively for (A) 0 day, (B) 12 days,

15

(C) 30 days, (D) 60 days.

16



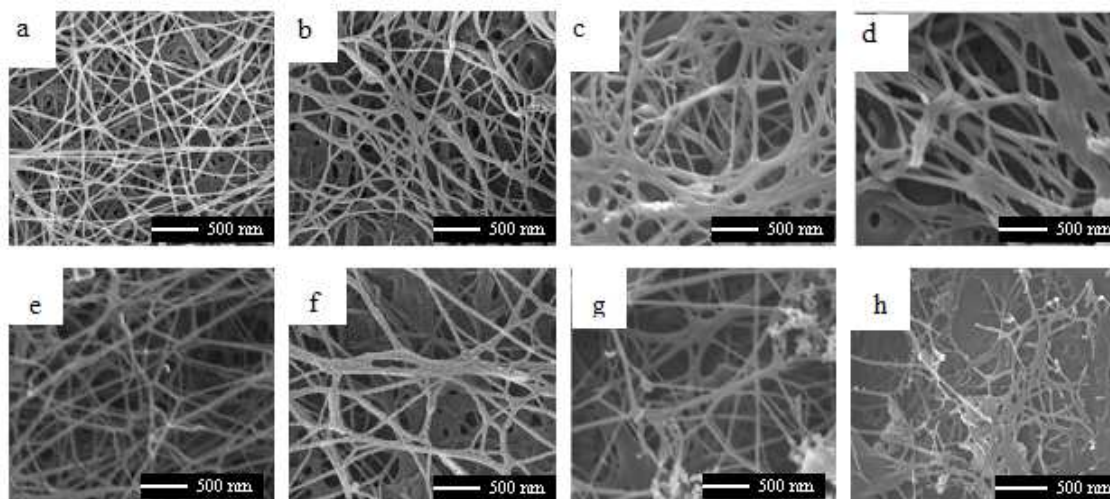
17

18

19 Fig.4. XRD patterns of (a)BC and (b)OBC immersed in PBS for (A)0 day, (B)12 day, (C)30 days,

20

(D)60 days.

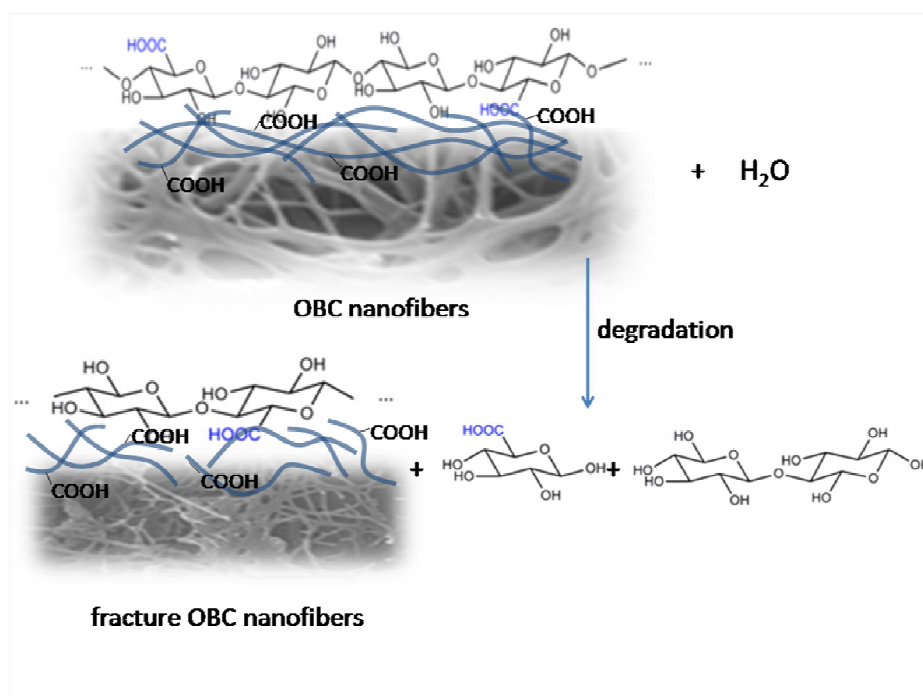


21

22

23 Fig.5. SEM of BC and OBC before (a, b, c, d) and after (e, f, g, h, corresponding to a, b, c, d  
 24 respectively) degradation for 60days (a)BC, (b) OBC oxidized for 3 days, (c) 6 days, (d) 12 days.

25

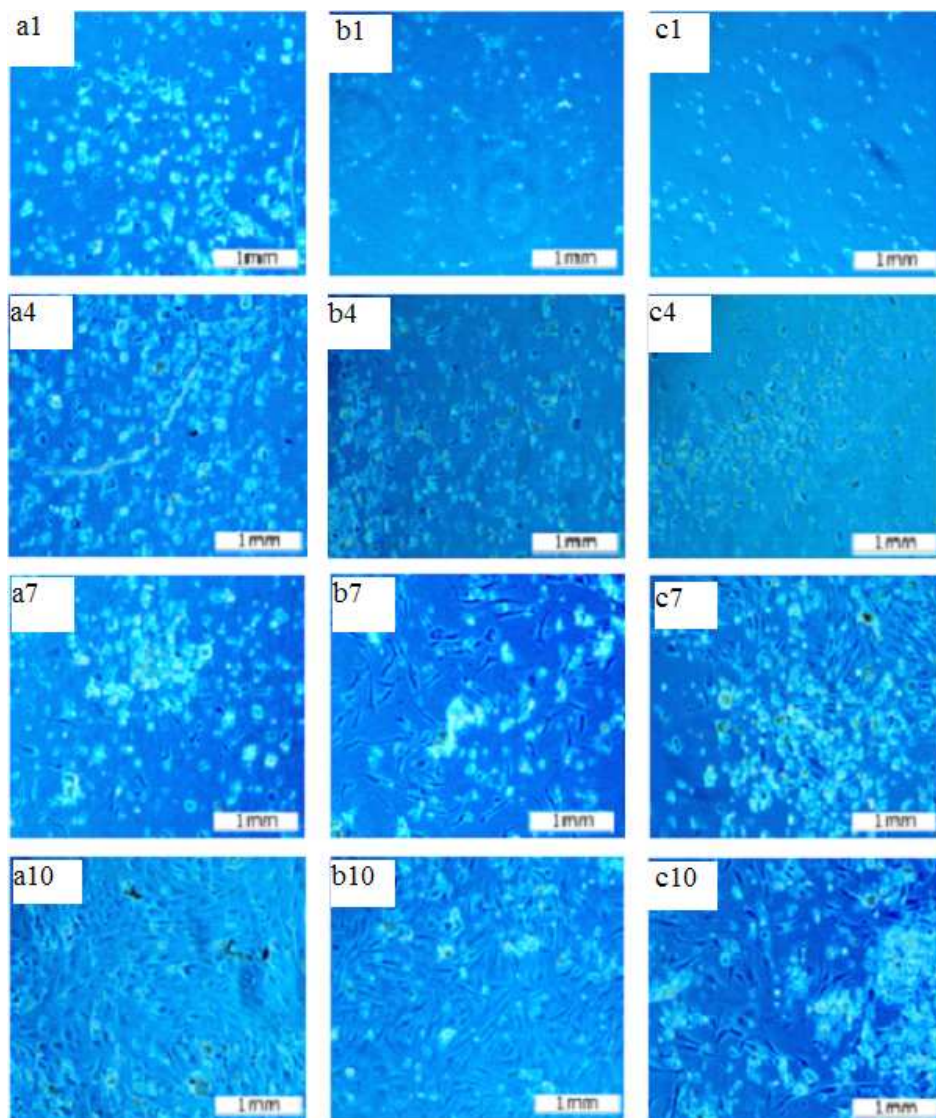


26

27

28 Fig.6 Degradation and breaking of OBC molecule chains

28



29

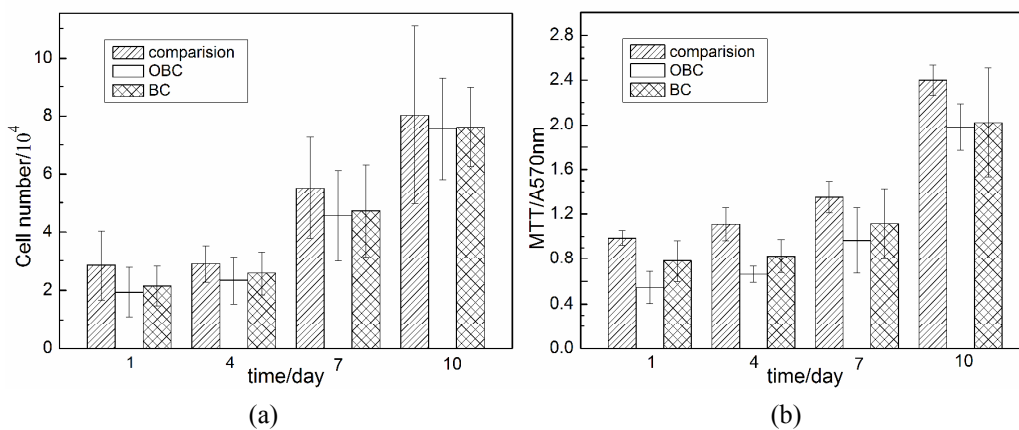
30 Fig.7 Optical photos of proliferation status (cytomorphology) of epidermal cells after cultivation

31 with different samples (a: blank control, b: OBC and c: BC): a1, b1 and c1 for 1 day; a4, b4 and c4

32 for 4 days; a7, b7 and c7 for 7 days; a10, b10 and c10 for 10 days.

33





34

35

36

37

38

Fig.8 Cellular affinity of OBC compared with blank control and BC (a) epidermal cell numbers during the proliferation, (b) MTT of cells cultivated with different materials.